Journal of Nonlinear Modeling and Analysis
Volume 7, Number 6, December 2025, 2157–2181
https://journal.global-sci.org/jnma
DOI:10.12150/jnma.2025.2157

Spatiotemporal Dynamics of a Memory-Diffusion Predator-Prey System with Two Delays and Nonlocal Competition*

Xu Wen[1] and Yuting Ding[1,†]

Abstract Predator gestation delay and memory period, along with nonlocal competition, play key roles in controlling population density and maintaining the stability of ecosystems. To control the population density of the Dendrolimus superans, which causes significant damage to forests, we propose a pest control system incorporating both two delays and nonlocal competition considering Holling II type functional response. We analyze the conditions for the existence of Hopf bifurcation and derive the normal form of Hopf bifurcation using multiple time scales method. Considering the biological significance, we employ appropriate parameters for numerical simulations. Furthermore, we find that varying habitat complexity parameters leads to different moduli of bifurcation periodic solutions. Especially, both two delays contribute to maintaining the stability of steady states.

Keywords Pest control model, two delays, Hopf bifurcation, nonlocal competition, habitat complexity

MSC(2010) 35B32, 35B35, 35Q92.

1. Introduction

The Dendrolimus superans, a common forest pest, is widely distributed worldwide. Dendrolimus superans is found in Siberia and the Far East of Russia, northern Mongolia, northern Korea, China, and Japan. Due to its widespread distribution, rapid spread and strong reproductive capability, Dendrolimus superans causes significant damage to agriculture and forestry economies. The Dendrolimus superans primarily infests coniferous trees such as larch, pine, and spruce, with its larvae extensively feeding and causing severe damage to the trees, ultimately leading to widespread destruction and even large-scale mortality. It exhibits a cyclical pattern of outbreaks and is difficult to control, resulting in significant economic losses to the local agriculture and forestry sectors. Furthermore, the extensive reproduction and feeding of Dendrolimus superans disrupt the ecological balance of local forest ecosystems, impacting the survival and reproduction of other biological populations. The life cycle of the Dendrolimus superans consists of four stages: egg, larva, pupa,

†the corresponding author.
Email address: 1812628478@qq.com (Xu Wen), yuting840810@163.com (Yuting Ding)
[1]Department of Mathematics, Northeast Forestry University, No. 26 Hexing Road, Heilongjiang 150040, China
*The authors were supported by the National Natural Science Foundation of China (No. 12571525).

and adult, with the larval stage being the most destructive to forests. The spread mechanism of the Dendrolimus superans is illustrated in Fig.1: female moths exhibit a tendency to oviposit in healthy forest stands; however, in cases of poor stand health, they will migrate to adjacent healthy stands. (In the figure, the darker trees represent unhealthy trees, while the lighter trees represent healthy trees.)

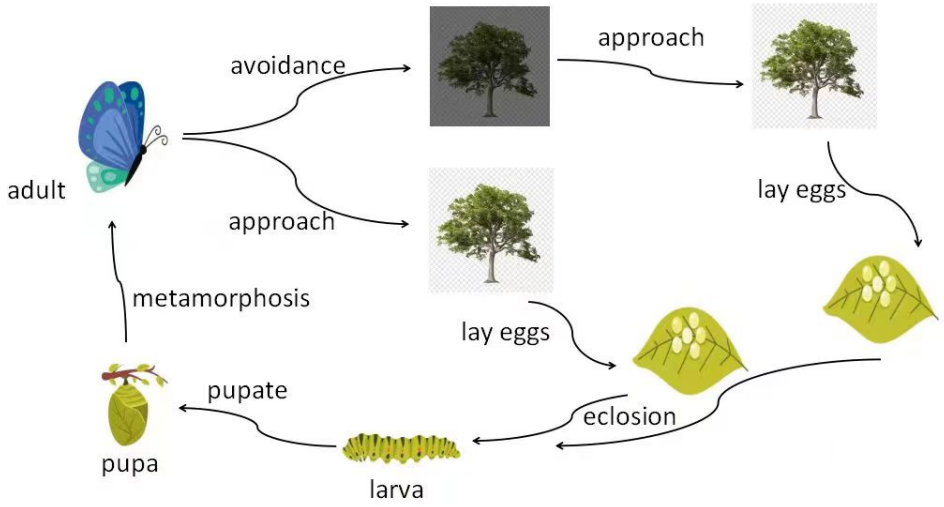

Figure 1. Spread mechanism of Dendrolimus superans infestation.

Three main methods are employed for the prevention and control of the Dendrolimus superans: physical control, chemical control, and biological control. Physical control primarily targets the behavioral patterns and characteristics of the Dendrolimus superans. It involves manual and simple tool interventions when the infestation area is small. However, this method requires a significant amount of manpower and resources, making it unsuitable for large-scale control of the Dendrolimus superans. Chemical control, on the other hand, is effective for large-scale infestations. Pesticides and other chemical agents are used to control the Dendrolimus superans [1]. Despite significant improvements in chemical control methods, they still pose certain risks to forest ecosystems and contribute to environmental pollution. Considering the principles of sustainable development and minimizing environmental damage, there is a growing interest in biological control. The natural enemies of the Dendrolimus superans can be classified into two categories: parasitic and predatory enemies. Parasitic enemies include species such as the Trichogrammatid and Tachinid fly, while predatory enemies include birds like the Parus cinereus and Garrulus glandarius, as illustrated in Fig.2.

In characterizing the relationship between the Dendrolimus superans and its natural enemies, we commonly employ predator-prey models, which are vital in the field of mathematical biology for studying the growth dynamics of two populations with predator-prey relationships. Scholars have continuously improved and refined these models in the past studies [2–7]. The flight range of adult female Dendrolimus superans is approximately 1 km, indicating limited dispersal ability. Hence, in

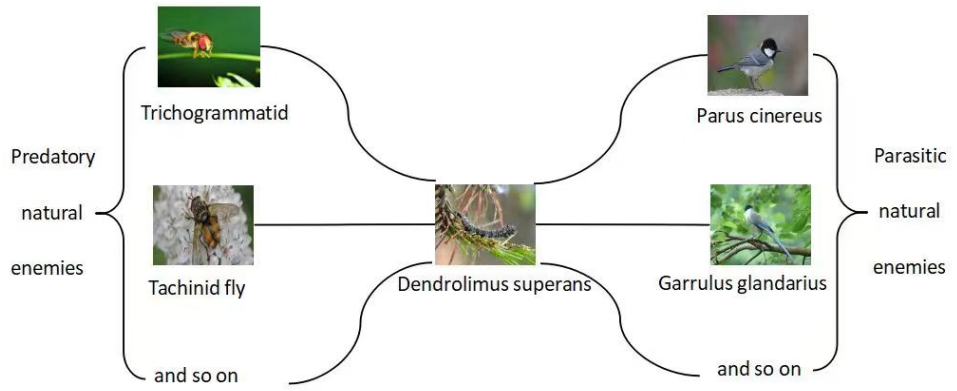

Figure 2. Different types of natural enemies of Dendrolimus superans.

the study of predator-prey models, the environment can be considered relatively closed. In such relatively closed natural environment, scholars focus on various factors that influence the overall system. Some biological studies suggest that habitat complexity affects population size and growth trends, highlighting its significant role in structuring ecological communities [8–10]. Additionally, the construction of mixed forests to provide habitats for natural enemies and enhance environmental complexity can effectively control the population of Dendrolimus superans [11, 12]. Therefore, studying the biological control of Dendrolimus superans and its impact on forest ecosystems by using mathematical models is meaningful. Since the introduction of the Lotka-Volterra model by Lotka in 1927 [13], it has been extensively studied in numerous fields [14, 15]. On the basis of Lotka-Volterra model, Ma and Wang [16] proposed a predator-prey model incorporating time delays and habitat complexity, that is

$$\begin{cases} \dfrac{du}{dt} = ru(1-\dfrac{u}{K}) - \dfrac{c(1-\beta)u^{\alpha}v}{1+ch(1-\beta)u^{\alpha}}, \\ \dfrac{dv}{dt} = \dfrac{ec(1-\beta)u^{\alpha}(t-\tau)v(t-\tau)}{1+ch(1-\beta)u^{\alpha}(t-\tau)} - dv, \end{cases} \tag{1.1}$$

where u and v describe the population of prey and predator, respectively. r is the intrinsic growth rate of prey. K is the capacity of environmental for prey. c is the attack rate of predator. β stands for the strength of habitat complexity. h is the handling time of predator. e is the conversion efficiency. τ is the gestation delay of predator. d is the death rate of predator. α is a positive real number and represents a kind of aggregation efficiency. All parameters in the model are positive. Ma and Wang [16] hypothesized that predators undergo gestation delay.

In a relatively closed natural environment, the spatial distribution of predators and prey plays a crucial role in competition and resource utilization. Nonlocal competition captures the interactions between predators and prey at different spatial locations, thereby enabling more accurate predictions of population dynamics and

competitive outcomes. Wu and Song [17] derived the normal forms of steady states, Hopf bifurcations, and steady-Hopf bifurcations for a general reaction-diffusion model with nonlocal effects and delays. Peng and Zhang [18] considered a predator-prey model with collective behavior and nonlocal prey competition, concluding that nonlocal competition disrupts the stability of the predator-prey system.

Besides factors such as space and environment, time also plays a crucial role in the stability of the entire system. Gestation delay and memory period play crucial roles in predator-prey systems. For predators, gestation delay refers to the time interval between predation and egg-laying or offspring production. During this delay, predators may not be able to prey again or their hunting ability may be restricted. The length of gestation delay directly impacts the predation efficiency of individual predators and the population growth rate. Refs. [19–22] established a kind of predator-prey models with gestation delay, and analyzed the dynamic properties of the models.

Predators can use memory in prey capture decisions to optimize hunting strategies, such as avoiding toxic prey or selecting appropriate times and locations for predation. The presence of memory period influences both the predator's hunting success rate and the dynamic evolution of prey populations, thereby introducing nonlinear effects and complex dynamic behaviors in predator-prey systems. Lv [23] proposed a diffusion system with a memory period and general delay by incorporating a reaction term into a memory-based diffusion system. Wang et al. [24] proposed and analyzed a diffusive predator-prey model with memory-based dynamics. Their study suggests that the memory period may induce Hopf bifurcation, leading to spatially heterogeneous periodic solutions. In summary, both gestation delay and memory period are significant factors influencing predator-prey interactions. They introduce additional complexity and nonlinearity into models, allowing for a more accurate description of the dynamic processes of predator-prey systems in natural environments.

Gestation delay and memory period are indispensable components of a predator's hunting process. Food acquisition directly impacts population reproduction, thus influencing population density. For instance, an increase in predator pregnancy delays reduces offspring reproduction, leading to a decrease in population density. Similarly, prolonging the memory cycle decreases the amount of food predators acquire, resulting in a reduction in predator numbers and an increase in prey abundance. As predators of the rapidly reproducing Dendrolimus superans, there is significant research value in studying the delays in both aspects. Thus, the correct utilization of biological pest control becomes pivotal in refining and improving this model.

Inspired by the above, we incorporate nonlocal competition, gestation delay and memory period into model (1.1) as follows:

$$\begin{cases} \dfrac{\partial u(x,t)}{\partial t} = d_1\Delta u + ru\left(1-\dfrac{\widetilde{u}}{K}\right) - \dfrac{acuv}{1+achu}, x\in\Omega,\ t>0, \\ \dfrac{\partial v(x,t)}{\partial t} = d_2\Delta v + \dfrac{gacu(x,t-\tau_1)v(x,t-\tau_1)}{1+achu(x,t-\tau_1)} - dv - d_3\nabla(v\nabla u(x,t-\tau_2)), x\in\Omega,\ t>0, \\ \dfrac{\partial u(x,t)}{\partial \overrightarrow{n}} = \dfrac{\partial v(x,t)}{\partial \overrightarrow{n}} = 0, x\in\partial\Omega,\ t>0, \\ u(x,t) = u_0(x,t)\geq 0,\ v(x,t) = v_0(x,t)\geq 0, \quad (t,x)\in[-\tau,0]\times\overline{\Omega}, \quad \tau = \max\{\tau_1,\tau_2\}, \end{cases} \tag{1.2}$$

where u and v describe the density of Dendrolimus superans (prey) and natural enemy (predator), respectively. r is the birth rate of Dendrolimus superans. K is the capacity of environmental for Dendrolimus superans. d_1 and d_2 stand for the diffusion coefficients of Dendrolimus superans and natural enemy, respectively. g is the energy transfer efficiency from Dendrolimus superans to predator. a is the attack rate of predator on prey. c is the stength of habitat complexity. h is the handing time. d stands for the death rate of natural enemy. d_3 is the memory-diffusion coefficient of predator. τ_1 is the gestation delay of natural enemy. τ_2 is the memory period of natural enemy. $r, K, a, c, h, g, d, d_1, d_2, d_3$ are all positive constants. We select $\Omega = (0, l\pi)$, where $l > 0$. $\widetilde{u} = \frac{1}{K}\int_\Omega G(x,y)u(y,t)dy$ represents the nonlocal competition, and the kernel function is given by $G(x,y) = \frac{1}{|\Omega|} = \frac{1}{l\pi}$. This is based on the assumption that the competition intensity among prey individuals in the habitat is uniform, meaning that the competition between any two preys is identical. The boundary condition is the Newman boundary, which can be interpreted as the habitat of the population being closed, where no prey or predator can enter or leave the habitat. This study aims to investigate the dynamics of predator-prey model, focusing particularly on the dynamics of system stability and dynamic properties as the time delay parameter serves as the bifurcation parameter and varies.

The remaining sections of this paper are organized as follows. Section 2 examines the stability of positive constant steady states and the existence of Hopf bifurcation. Section 3 investigates the properties of Hopf bifurcation. Section 4 presents numerical simulations. Finally, conclusions are drawn in Section 5.

2. Stability analysis

The model (1.2) has an unstable constant steady state $E_0 = (0, 0)$ and we make the following hypothesis:

$$(H_0)\ g > hd, d < Kac(g - hd).$$

If (H_0) is satisfied, then the model (1.2) has a positive constant steady state $E_1 = (u_*, v_*)$, where

$$u_* = \frac{d}{(g-hd)ac}, v_* = \frac{rg}{(g-hd)ac}\Big(1 - \frac{u_*}{K}\Big).$$

Linearizing model (1.2) at $E_1 = (u_*, v_*)$, we obtain

$$\frac{\partial}{\partial t}U = D\begin{pmatrix}\Delta u(x,t)\\ \Delta v(x,t)\end{pmatrix} + L_1\begin{pmatrix}\Delta u(x,t-\tau_2)\\ \Delta v(x,t-\tau_2)\end{pmatrix} + L_2\begin{pmatrix}u(x,t)\\ v(x,t)\end{pmatrix} + L_3\begin{pmatrix}u(x,t-\tau_1)\\ v(x,t-\tau_1)\end{pmatrix} + L_4\begin{pmatrix}\widetilde{u}(x,t)\\ \widetilde{v}(x,t)\end{pmatrix},$$

where

$$D = \begin{pmatrix}d_1 & 0\\ 0 & d_2\end{pmatrix}, L_1 = \begin{pmatrix}0 & 0\\ -d_3 v_* & 0\end{pmatrix}, L_2 = \begin{pmatrix}a_1 & a_2\\ 0 & -d\end{pmatrix}, L_3 = \begin{pmatrix}0 & 0\\ b_1 & b_2\end{pmatrix}, L_4 = \begin{pmatrix}c_1 & 0\\ 0 & 0\end{pmatrix},$$

with $a_1 = r(1 - \frac{u_*}{K})\frac{hd}{g} > 0$, $a_2 = -\frac{d}{g} < 0$, $b_1 = r(g - hd)(1 - \frac{u_*}{K}) > 0$, $b_2 = d > 0$, and $c_1 = -\frac{ru_*}{K} < 0$.

The characteristic equation of model (1.2), evaluated at $E_1 = (u_*, v_*)$ is given by

$$\lambda^2 + A_n\lambda + B_n + (C_n - d\lambda)\mathrm{e}^{-\lambda\tau_1} + D_n\mathrm{e}^{-\lambda\tau_2} = 0, n = 0, 1, 2\cdots, \tag{2.1}$$

where

$$\begin{cases} A_0 = d - a_1 - c_1, \\ B_0 = -a_1 d - c_1 d, \\ C_0 = a_1 b_2 + b_2 c_1 - a_2 b_1, \\ D_0 = 0, \end{cases}$$

and when $n \geq 1$, we have

$$\begin{cases} A_n = \left(\frac{n}{l}\right)^2 d_1 + \left(\frac{n}{l}\right)^2 d_2 + d - a_1, \\ B_n = \left(\frac{n}{l}\right)^4 d_1 d_2 + \left(\frac{n}{l}\right)^2 d_1 d - \left(\frac{n}{l}\right)^2 a_1 d_2 - a_1 d, \\ C_n = a_1 b_2 - a_2 b_1 - \left(\frac{n}{l}\right)^2 b_2 d_1, \\ D_n = -\left(\frac{n}{l}\right)^2 a_2 d_3 v_*. \end{cases}$$

2.1. The case for $\tau_1 = 0$, $\tau_2 = 0$

When $\tau_1 = \tau_2 = 0$, equation (2.1) becomes

$$\lambda^2 + (A_n - d)\lambda + B_n + C_n + D_n = 0, n = 0, 1, 2 \cdots . \tag{2.2}$$

Next, we analyze the conditions of habitat complexity that ensure the stability of positive constant steady state for the model (1.2).

If $A_0 - d = -(a_1 + c_1) > 0$, then it follows that $c < \frac{hd+g}{ahK(g-hd)}$. Because the function $A_n - d = (\frac{n}{l})^2(d_1 + d_2) - a_1$ is monotonically increasing, thus when $A_1 - d > 0$ holds, $A_n - d > 0$ holds for any $n \geq 1$. We have $A_1 - d = \frac{d_1+d_2}{l^2} - a_1 > 0$; it follows that $\frac{rhd^2}{gk(g-hd)ac} > \frac{rhdl^2-(d_1+d_2)g}{l^2 g}$. Thus, if $rhdl^2 - (d_1 + d_2)g > 0$, then $c \in \left(0, \frac{rhd^2 l^2}{Ka(g-hd)[rhdl^2-(d_1+d_2)g]}\right)$. Otherwise, if $rhdl^2 - (d_1 + d_2)g < 0$, then $c \in (0, +\infty)$. Define:

$$c_0 = \begin{cases} \dfrac{rhd^2 l^2}{Ka(g-hd)[rhdl^2 - (d_1+d_2)g]} & , rhdl^2 - (d_1 + d_2)g > 0, \\ \dfrac{hd+g}{ahK(g-hd)} & , rhdl^2 - (d_1 + d_2)g < 0. \end{cases}$$

Due to $a_2 < 0, b_1 > 0$, it follows that $B_0 + C_0 + D_0 = -a_2 b_1 > 0$ always holds. For $B_n + C_n + D_n = (\frac{n}{l})^4 d_1 d_2 - (\frac{n}{l})^2(a_1 d_2 + a_2 d_3 v_*) - a_2 b_1 > 0$, when $n = 0$, $-a_2 b_1 > 0$. Thus, when $\frac{a_1 d_2 + a_2 d_3 v_*}{2 d_1 d_2} \leq 0$ holds, $B_n + C_n + D_n > 0$ for any n, we have $\frac{a_1 d_2 + a_2 d_3 v_*}{2 d_1 d_2} \leq 0$; it follows that $c \leq \frac{d_3 g}{h d_2 a(g-hd)}$.

In summary, if $c < \min\{\frac{hd+g}{ahK(g-hd)}, \frac{d_3 g}{h d_2 a(g-hd)}, c_0\}$ holds, $A_0 - d > 0, A_n - d > 0$ and $B_n + C_n + D_n > 0$, for every $n \in \mathbb{N}$. Thus we make the following hypothesis

$$(H_1)\ c < \min\left\{\frac{hd+g}{ahK(g-hd)}, \frac{d_3 g}{h d_2 a(g-hd)}, c_0\right\}.$$

When (H_1) holds, the roots of characteristic equation (2.2) have negative real parts.

Theorem 2.1. *For model* (1.2) *with* $\tau_1 = \tau_2 = 0$, *if* (H_0) *and* (H_1) *hold, then the positive constant steady state* E_1 *of the model* (1.2) *is locally asymptotically stable.*

Remark 2.1. This means that habitat complexity is beneficial for controlling the stability of predator-prey models. Habitat complexity should be maintained within a certain range because $rhdl^2 - (d_1 + d_2)g$ indicates that when the habitat range l is sufficiently large, habitat complexity should be controlled within a specific range. At this point, excessive environmental complexity may have a certain impact on population stability. However, when the habitat range l is small, the requirement for habitat complexity to maintain population stability is not high.

2.2. The case for $\tau_1 \neq 0$, $\tau_2 = 0$

Next, we consider the existence of bifurcating periodic solutions near the positive constant steady state $E_1 = (u_*, v_*)$ for $\tau_1 > 0, \tau_2 = 0$. The characteristic equation of model (1.2) becomes

$$\lambda^2 + A_n\lambda + B_n + D_n + (C_n - d\lambda)\mathrm{e}^{-\lambda\tau_1} = 0, n = 0, 1, 2\cdots. \tag{2.3}$$

Let $\lambda = \pm i\omega$ ($i^2 = -1, \omega > 0$) be a root of characteristic equation (2.3). Substituting it into equation (2.3) and separating the real and imaginary parts, we obtain:

$$\begin{cases} -\omega^2 + B_n + D_n + C_n\cos(\omega\tau_1) - d\omega\sin(\omega\tau_1) = 0, \\ \omega A_n - C_n\sin(\omega\tau_1) - d\omega\cos(\omega\tau_1) = 0, \end{cases}$$

that is,

$$\begin{cases} \cos(\omega\tau_1) = \frac{\omega^2(dA_n + C_n) - (B_n + D_n)C_n}{C_n^2 + d^2\omega^2}, \\ \sin(\omega\tau_1) = \frac{\omega[A_nC_n + (B_n + D_n)d - d\omega^2]}{C_n^2 + d^2\omega^2}, \end{cases} \tag{2.4}$$

then for $j = 0, 1, 2, 3\cdots$ and $n = 0, 1, 2, 3\cdots$, we get

$$\tau_{1,n}^{(j)} = \begin{cases} \frac{1}{\omega}\arccos\big(\cos(\omega\tau_1)\big) + 2j\pi, & \sin(\omega\tau_1) \geq 0, \\ \frac{1}{\omega}\big[2\pi - \arccos\big(\cos(\omega\tau_1)\big)\big] + 2j\pi, & \sin(\omega\tau_1) < 0. \end{cases} \tag{2.5}$$

From (2.4), we obtain:

$$h(\omega^2) = \omega^4 + \omega^2[A_n^2 - 2(B_n + D_n) - d^2] + (B_n + D_n)^2 - C_n^2 = 0.$$

Let $z = \omega^2$. Then the above equation becomes

$$h(z) = z^2 + z[A_n^2 - 2(B_n + D_n) - d^2] + (B_n + D_n)^2 - C_n^2 = 0. \tag{2.6}$$

Calculating the transversality conditions, we have:

$$\mathrm{Re}\Big(\frac{d\lambda}{d\tau_1}\Big)^{-1}\Big|_{\tau_1 = \tau_{1,n}^{(j)}} = \frac{h'(z)}{C_n^2 + d^2z} = \frac{2z + A_n^2 - 2(B_n + D_n) - d^2}{C_n^2 + d^2z}.$$

Denote

$$\tau_{1,c}^* = \min\{\tau_{1,n}^{(j)} \big| n \in \mathbb{N}, j = 0, 1, 2, 3, \cdots\}, \tag{2.7}$$

and

$$\Delta_n = [A_n^2 - 2(B_n + D_n) - d^2]^2 - 4[(B_n + D_n)^2 - C_n^2], \tag{2.8}$$

where $\tau_{1,n}^{(j)}$ is given in Eq.(2.5).

Define that I_1 and I_2 are sets of integers, which may be finite or infinite,

$$I_1 = \{n_k \big| (B_{n_k} + D_{n_k})^2 - C_{n_k}^2 < 0, n_k \in \mathbb{N}\},$$

$$I_2 = \{n_t \big| A_{n_t}^2 - 2(B_{n_t} + D_{n_t}) - d^2 < 0, (B_{n_t} + D_{n_t})^2 - C_{n_t}^2 > 0, \Delta_{n_t} > 0, n_t \in \mathbb{N}\},$$

where Δ_{n_t} is given in Eq.(2.8).

When $I_1 \neq \emptyset$ holds, Eq.(2.6) has a unique positive root z_{n_k} for some $n = n_k \in I_1$. Therefore, we can solve for ω_{n_k} and $\tau_{1,n_k}^{(j)}$, where

$$\omega_{n_k} = \sqrt{\frac{1}{2}\Big[- [A_{n_k}^2 - 2(B_{n_k} + D_{n_k}) - d^2] + \sqrt{\Delta_{n_k}}\Big]}.$$

Since $h'(z_{n_k}) > 0$, we have $\mathrm{Re}\big(\frac{d\lambda}{d\tau_1}\big)^{-1}\Big|_{\tau_1=\tau_{1,n_k}^{(j)}} > 0$.

When $I_2 \neq \emptyset$ holds, Eq.(2.6) has two positive roots $z_{n_t,i}$ for some $n = n_t \in I_2$, $i = 1, 2$. Therefore, we can solve for $\omega_{n_t,i}$ and $\tau_{1,n_t,i}^{(j)}$, $i = 1, 2$, where

$$\begin{cases} \omega_{n_t,1} = \sqrt{\frac{1}{2}\Big[- [A_{n_t,1}^2 - 2(B_{n_t,1} + D_{n_t,1}) - d^2] - \sqrt{\Delta_{n_t,1}}\Big]}, \\ \omega_{n_t,2} = \sqrt{\frac{1}{2}\Big[- [A_{n_t,2}^2 - 2(B_{n_t,2} + D_{n_t,2}) - d^2] + \sqrt{\Delta_{n_t,2}}\Big]}. \end{cases}$$

Due to $\omega_{n_t,1} < \omega_{n_t,2}$, we have $h'(z_{n_t,1}) < 0$ and $h'(z_{n_t,2}) > 0$. Thus

$$\mathrm{Re}\big(\frac{d\lambda}{d\tau_1}\big)^{-1}\Big|_{\tau_1=\tau_{1,n_t,1}^{(j)}} < 0, \mathrm{Re}\big(\frac{d\lambda}{d\tau_1}\big)^{-1}\Big|_{\tau_1=\tau_{1,n_t,2}^{(j)}} > 0$$

holds.

Based on the above results, we can derive the following conclusions.

Theorem 2.2. *Considering model* (1.2) *with* $\tau_1 > 0$ *and* $\tau_2 = 0$, *and assuming* (H_0) *and* (H_1) *hold,* $\tau_{1,n}^{(j)}$ *is given in Eq.*(2.5). *Thus, we have the following conclusions:*

(i) If $I_1 = \emptyset$ *and* $I_2 = \emptyset$, *Eq.*(2.6) *has no positive roots, then the positive constant steady state* E_1 *is always locally asymptotically stable for* $\tau_1 > 0$;

(ii) If $I_1 \neq \emptyset$ *and* $I_2 = \emptyset$, *then Eq.*(2.6) *has a unique positive root* z_{n_k} *for some* $n_k \in I_1$, *then the positive constant steady state* E_1 *of the model* (1.2) *is asymptotically stable for* $0 < \tau_1 < \tau_{1,c}^*$ *and unstable for* $\tau_1 > \tau_{1,c}^*$, *where* $\tau_{1,c}^* = \min\{\tau_{1,n_k}^{(0)} \big| n_k \in I_1\}$. *Moreover, the model* (1.2) *undergoes* n_k*-mode Hopf bifurcation near the positive constant steady state* E_1 *for* $\tau_1 = \tau_{1,n_k}^{(j)}$ *with* $n_k \in I_1$ *and* $j = 0, 1, 2, 3 \cdots$;

(iii) If $I_1 = \emptyset$ *and* $I_2 \neq \emptyset$, *then Eq.*(2.6) *has two positive roots* $z_{n_t,i} (i = 1, 2)$ *for some* $n_t \in I_2$, *then the positive constant steady state* E_1 *of the model* (1.2) *is asymptotically stable for* $0 < \tau_1 < \tau_{1,c}^*$, *and there may be a switch of stability for* $\tau_1 > \tau_{1,c}^*$ *in the model* (1.2), *where* $\tau_{1,c}^* = \min\{\tau_{1,n_t}^{(0)} \big| n_t \in I_2\}$. *Moreover, the model* (1.2) *undergoes* n_k*-mode Hopf bifurcation near the positive constant steady state* E_1 *for* $\tau_1 = \tau_{1,n_t}^{(j)}$ *with* $n_t \in I_2$ *and* $j = 0, 1, 2, 3 \cdots$;

(iv) If $I_1 \neq \emptyset$ and $I_2 \neq \emptyset$, then Eq.(2.6) *has positive roots z_{n_k} and $z_{n_t,i}(i = 1, 2)$. Denote that n_p corresponds to the smallest critical time delay $\tau^*_{1,c}$, where $n_p \in I_1$ or $n_p \in I_2$. Then the positive constant steady state E_1 of the model* (1.2) *is asymptotically stable for $0 < \tau_1 < \tau^*_{1,c}$, and there may be a switch of stability for $\tau_1 > \tau^*_{1,c}$ in the model* (1.2)*, where $\tau^*_{1,c} = \min\{\tau^{(0)}_{1,n_p} | n_p \in I_1,$ or $n_p \in I_2\}$. Moreover, the model* (1.2) *undergoes n_p-mode Hopf bifurcation near the positive constant steady state E_1 for $\tau_1 = \tau^{(j)}_{1,n_p}$ with $n_p \in I_1$, or $n_p \in I_2$ and $j = 0, 1, 2, 3 \cdots$.*

2.3. The case for $\tau_1 \neq 0$,$\tau_2 \neq 0$

Finally, we denote the first stable interval associated with τ_1 mentioned in Theorem 2.2 as I, on which the positive constant steady state $E_1 = (u_*, v_*)$ is locally asymptotically stable. Next, we choose $\tau_1 = \tau^*_1 \in I$. Regarding τ_2 as a parameter, because characteristic equation of model (1.2) at $E_1 = (u_*, v_*)$ is consistent with the equation (2.3) for $n = 0$. Therefore, we only consider the case when $n = 1, 2, 3 \cdots$, the characteristic equation of model (1.2) at $E_1 = (u_*, v_*)$ is rewritten as follows:

$$\lambda^2 + (A_n - d\mathrm{e}^{-\lambda\tau^*_1})\lambda + D_n\mathrm{e}^{-\lambda\tau_2} + C_n\mathrm{e}^{-\lambda\tau^*_1} + B_n = 0, n = 1, 2 \cdots . \tag{2.9}$$

Let $\lambda = \pm i\omega_2$ ($i^2 = -1, \omega_2 > 0$) be a root of characteristic equation (2.9). Substituting the root into equation (2.9) and separating the real and imaginary parts, we obtain:

$$\begin{cases} \omega_2^2 - B_n - C_n\cos(\omega_2\tau^*_1) + d\omega_2\sin(\omega_2\tau^*_1) = D_n\cos(\omega_2\tau_2), \\ A_n\omega_2 - C_n\sin(\omega_2\tau^*_1) - d\omega_2\cos(\omega_2\tau^*_1) = D_n\sin(\omega_2\tau_2), \end{cases} \tag{2.10}$$

that is

$$\begin{cases} \cos\omega_2\tau_2 = \frac{\omega_2^2 - B_n - C_n\cos(\omega_2\tau^*_1) + d\omega_2\sin(\omega_2\tau^*_1)}{D_n}, \\ \sin\omega_2\tau_2 = \frac{A_n\omega_2 - C_n\sin(\omega_2\tau^*_1) - d\omega_2\cos(\omega_2\tau^*_1)}{D_n}, \end{cases} \tag{2.11}$$

which leads to

$$\begin{aligned} F(\omega_2) =& \omega_2^4 + (A_n^2 - d^2 - 2B_n)\omega_2^2 + 2(-dB_n\omega_2 - A_nC_n\omega_2 + d\omega_2^3)\sin\omega_2\tau^*_1 \\ &+ C_n^2 + B_n^2 - D_n^2 + 2(C_nB_n - A_nd\omega_2^2 - C_n\omega_2^2)\cos\omega_2\tau^*_1 = 0. \end{aligned} \tag{2.12}$$

Define the following set (finite or infinite)

$$I_3 = \{n_{s_1}, n_{s_2}, \cdots, n_{s_m}, \cdots\} \in \mathbb{N},$$

such that the equation (2.12) has positive roots for $n = n_s \in I_3$. Thus, $F(\omega_2) = 0$ has definite positive roots ω_{n_s}. For every fixed ω_{n_s}, there is a sequence of $\tau^{(j)}_{2,n_s}, j = 0, 1, 2 \cdots$, defined by

$$\tau^{(j)}_{2,n_s} = \begin{cases} \frac{1}{\omega_2}\arccos\big(\cos(\omega_2\tau_2)\big) + 2j\pi, & \sin(\omega_2\tau_2) \geq 0, \\ \frac{1}{\omega_2}\big[2\pi - \arccos\big(\cos(\omega_2\tau_2)\big)\big] + 2j\pi, & \sin(\omega_2\tau_2) < 0. \end{cases} \tag{2.13}$$

Denote

$$\tau_c = \min\{\tau^{(j)}_{2,n_s} | n_s \in \mathbb{N}, j = 0, 1, 2, 3, \cdots\}, \tag{2.14}$$

and

$$(H_2)\ \mathrm{Re}\Big(\frac{d\lambda}{d\tau_2}\Big)^{-1}_{\tau_2=\tau^{(j)}_{2,n_s}} \neq 0.$$

Then we have the following statements.

Theorem 2.3. *Assume that* (H_0), (H_1) *and* (H_2) *are satisfied, and that one of the cases in Theorem 2.2 holds. If* $I_3 \neq \emptyset$, *then for* $\tau_1^* \in I$, *model* (1.2) *has positive roots* ω_{n_s} *for some* $n = n_s$, *then the positive constant steady state* E_1 *of the model* (1.2) *is asymptotically stable for* $0 < \tau_2 < \tau_c$ *and unstable for* $\tau_2 > \tau_c$, *where* $\tau_c = \min\{\tau_{2,n_s}^{(0)} | n_s \in I_3\}$. *Moreover, the model* (1.2) *undergoes* n_s*-mode Hopf bifurcation near the positive constant steady state* E_1 *for* $\tau_2 = \tau_{2,n_s}^{(j)}$ *with* $n_s \in I_3$ *and* $j = 0, 1, 2, 3 \cdots$.

3. Normal form of Hopf bifurcation

In this section, we derive the normal form of Hopf bifurcation of model (1.2) by using multiple time scales method. For $\tau_1^* \in I$, when $\tau_2 = \tau_c$, the characteristic equation (2.9) has a pair of pure imaginary roots $\pm i\omega$, at which model (1.2) undergoes n_s-mode Hopf bifurcation at the positive constant steady state $E_1 = (u_*, v_*)$, τ_c is given in Eq.(2.14). In the following derivation, we use n instead of n_s for simplicity. In order to study the impact of the time required for predators to initiate hunting based on their own memory of prey, during the pursuit of prey, we treat time delay τ_2 as a bifurcation parameter, where $\tau_2 = \tau_c + \varepsilon\mu$, with $\tau_2 = \tau_c$ being the critical value for Hopf bifurcation. The parameter ε is a dimensionless scaling factor, and μ is a perturbation parameter. In order to normalize the delay, we set $u(x,t) \to u(x,t) - u_*$, $v(x,t) \to v(x,t) - v_*$; then model (1.2) can be rewritten as

$$\begin{cases} \dfrac{\partial u(x,t)}{\partial t} = & d_1\Delta u + u\Big(r - f_1 - \dfrac{u_*}{K}\Big) - \Big(\dfrac{u+u_*}{K}\Big)\widetilde{u} - f_2 v - \dfrac{1}{2}f_{11}u^2 - f_{12}uv \\ & - \dfrac{1}{6}f_{111}u^3 - \dfrac{1}{2}f_{112}u^2 v, \\ \dfrac{\partial v(x,t)}{\partial t} = & d_2\Delta u - d_3(v+v_*)u_{xx}(x,t-\tau_2) - d_3 v_x u_x(x,t-\tau_2) + g f_2 v(x,t-\tau_1) \\ & + g f_1 u(x,t-\tau_1) + \dfrac{g}{2}f_{11}u^2(x,t-\tau_1) + g f_{12}u(x,t-\tau_1)v(x,t-\tau_1) \\ & + \dfrac{g}{6}f_{111}u^3(x,t-\tau_1) - dv + \dfrac{g}{2}f_{112}u^2(x,t-\tau_1)v(x,t-\tau_1), \end{cases} \tag{3.1}$$

where

$$f_1 = \frac{acv_*}{(1+achu_*)^2}, f_2 = \frac{acu_*}{1+achu_*}, f_{11} = -\frac{2(ac)^2 hv_*}{(1+achu_*)^3},$$
$$f_{12} = \frac{ac}{(1+achu_*)^2}, f_{111} = \frac{6(ac)^3 h^2 v_*}{(1+achu_*)^4}, f_{112} = -\frac{2(ac)^2 h}{(1+achu_*)^3}.$$

Let $h = (h_{11}, h_{12})^T$ be the eigenvector of the linear operator of system (3.1) corresponding to the eigenvalue $i\omega$, and let $h^* = (h_{11}^*, h_{12}^*)^T$ be the normalized eigenvector of the adjoint operator of the linear operator of system (3.1) corresponding to the eigenvalues $-i\omega$ satisfying the inner product $< h^*, h >= \overline{h^*}^T \cdot h = 1$. By a simple calculation, we get

$$\begin{aligned} h &= (h_{11}, h_{12})^T = \Big(1, \frac{-i\omega - (\frac{n}{l})^2 d_1 + r - f_1 - \frac{u_*}{K} - \frac{u_*}{K}x_n}{f_2}\Big), \\ h^* &= q(h_{21}, h_{22})^T = q\Big(\frac{f_2}{i\omega - (\frac{n}{l})^2 d_1 + r - f_1 - \frac{u_*}{K} - \frac{u_*}{K}x_n}, 1\Big), \end{aligned} \tag{3.2}$$

with $q = (\overline{h_{11}}h_{21} + h_{22}\overline{h_{12}})^{-1}$, and

$$x_n = \begin{cases} 1, n = 0, \\ 0, n \neq 0. \end{cases}$$

Suppose that the solution of Eq.(3.1) is

$$U(x,t) = U(x,T_0,T_1,T_2,\cdots) = \sum_{k=1}^{+\infty} \varepsilon^k U_k(x,T_0,T_1,T_2,\cdots), \tag{3.3}$$

where

$$U(x,T_0,T_1,T_2,\cdots) = (u(x,T_0,T_1,T_2,\cdots), v(x,T_0,T_1,T_2,\cdots))^T,$$
$$U_k(x,T_0,T_1,T_2,\cdots) = (u_k(x,T_0,T_1,T_2,\cdots), v_k(x,T_0,T_1,T_2,\cdots))^T.$$

The derivation with respect to t is

$$\frac{\partial}{\partial t} = \frac{\partial}{\partial T_0} + \varepsilon \frac{\partial}{\partial T_1} + \varepsilon^2 \frac{\partial}{\partial T_2} + \cdots = D_0 + \varepsilon D_1 + \varepsilon^2 D_2 + \cdots,$$

where the differential operator $D_i = \frac{\partial}{\partial T_i}, i = 0,1,2,\cdots$.

We obtain

$$\begin{cases} \dfrac{\partial U(x,t)}{\partial t} = \varepsilon D_0 U_1 + \varepsilon^2 D_0 U_2 + \varepsilon^2 D_1 U_1 + \varepsilon^3 D_0 U_3 + \varepsilon^3 D_1 U_2 + \varepsilon^3 D_2 U_1 + \cdots, \\ \Delta U(x,t) = \varepsilon \Delta U_1(x,t) + \varepsilon^2 \Delta U_2(x,t) + \varepsilon^3 \Delta U_3(x,t) + \cdots. \end{cases} \tag{3.4}$$

Denote

$$u_j = u_j(x,T_0,T_1,T_2,\cdots), v_j = v_j(x,T_0,T_1,T_2,\cdots),$$

and

$$u_{j,\tau_1} = u_j(x,T_0-\tau_1,T_1,T_2,\cdots), v_{j,\tau_1} = v_j(x,T_0-\tau_1,T_1,T_2,\cdots),$$
$$u_{j,\tau_c} = u_j(x,T_0-\tau_c,T_1,T_2,\cdots), v_{j,\tau_c} = v_j(x,T_0-\tau_c,T_1,T_2,\cdots),$$

with $j = 1,2,3,\cdots$.

We take perturbations as $\tau_2 = \tau_c + \varepsilon\mu$ to deal with the delayed terms. By expending $U(x,t-\tau_1)$ and $U(x,t-\tau_2)$ at $U(x,T_0-\tau_1,T_1,T_2,\cdots)$ and $U(x,T_0-\tau_2,T_1,T_2,\cdots)$, respectively, we have

$$\begin{cases} u(x,t-\tau_1) = \varepsilon u_{1,\tau_1} + \varepsilon^2(u_{2,\tau_1} - \tau_1 D_1 u_{1,\tau_1}) + \varepsilon^3(u_{3,\tau_1} - \tau_1 D_1 u_{2,\tau_1} - \tau_1^2 D_2 u_{1,\tau_1}) \\ \qquad\qquad + \cdots, \\ v(x,t-\tau_1) = \varepsilon v_{1,\tau_1} + \varepsilon^2(v_{2,\tau_1} - \tau_1 D_1 v_{1,\tau_1}) + \varepsilon^3(v_{3,\tau_1} - \tau_1 D_1 v_{2,\tau_1} - \tau_1^2 D_2 v_{1,\tau_1}) \\ \qquad\qquad + \cdots, \\ u(x,t-\tau_2) = \varepsilon u_{1,\tau_c} + \varepsilon^2 u_{2,\tau_c} + \varepsilon^3 u_{3,\tau_c} - \varepsilon^2\mu D_0 u_{1,\tau_c} - \varepsilon^3\mu D_0 u_{2,\tau_c} - \varepsilon^2\tau_c D_1 u_{1,\tau_c} \\ \qquad\qquad - \varepsilon^3\mu D_1 u_{1,\tau_c} - \varepsilon^3\tau_c D_2 u_{1,\tau_c} - \varepsilon^3\tau_c D_1 u_{2,\tau_c} + \cdots, \\ v(x,t-\tau_2) = \varepsilon v_{1,\tau_c} + \varepsilon^2 v_{2,\tau_c} + \varepsilon^3 v_{3,\tau_c} - \varepsilon^2\mu D_0 v_{1,\tau_c} - \varepsilon^3\mu D_0 v_{2,\tau_c} - \varepsilon^2\tau_c D_1 v_{1,\tau_c} \\ \qquad\qquad - \varepsilon^3\mu D_1 v_{1,\tau_c} - \varepsilon^3\tau_c D_2 v_{1,\tau_c} - \varepsilon^3\tau_c D_1 v_{2,\tau_c} + \cdots. \end{cases} \tag{3.5}$$

Substituting Eqs.(3.3)-(3.5) into Eq.(3.1), for the ε-order terms, we obtain

$$\begin{cases} D_0u_1 - d_1u_{xx,1} - \Big(r - f_1 - \dfrac{u_*}{K}\Big)u_1 + \dfrac{u_*}{K}\widetilde{u_1} + f_2v_1 = 0, \\ D_0v_1 - d_2v_{xx,1} + d_3v_*u_{xx,1,\tau_c} - gf_2v_{1,\tau_1} - gf_1u_{1,\tau_1} + dv_1 = 0. \end{cases} \tag{3.6}$$

Since $\pm i\omega$ is the eigenvalues of the linear operator of Eq.(3.1), the solution of Eq.(3.6) can be expressed in the following form

$$U_1(x, T_0, T_1, T_2, \cdots) = G(T_1, T_2, \cdots)\mathrm{e}^{i\omega T_0}h\cos\Big(\frac{nx}{l}\Big) + c.c., \tag{3.7}$$

where c.c. means the complex conjugate of the preceding terms, and h is given in Eq.(3.2).

For ε^2, we obtain

$$\begin{cases} \quad D_0u_2 - d_1u_{xx,2} - \Big(r - f_1 - \dfrac{u_*}{K}\Big)u_2 + \dfrac{u_*}{K}\widetilde{u_2} + f_2v_2 \\ = - D_1u_1 - \dfrac{\widetilde{u_1}v_1}{K} - \dfrac{1}{2}f_{11}u_1^2 - f_{12}u_1v_1, \\ \quad D_0v_2 - d_2v_{xx,2} + d_3v_*u_{xx,2,\tau_c} - gf_2v_{2,\tau_1} - gf_1u_{2,\tau_1} + dv_2 \\ = - D_1v_1 - d_3u_{xx,1,\tau_c}v_1 + d_3v_*\mu D_0u_{xx,1,\tau_c} + d_3v_*\tau_cD_1u_{xx,1,\tau_c} - d_3u_{x,1,\tau_c}v_{x,1} \\ \quad - gf_2\tau_1D_1v_{1,\tau_1} - gf_1\tau_1D_1u_{1,\tau_1} + \dfrac{g}{2}f_{11}u_{1,\tau_1}^2 + gf_{12}u_{1,\tau_1}v_{1,\tau_1}. \end{cases} \tag{3.8}$$

Substituting Eq.(3.7) into the right-hand side of Eq.(3.8), we obtain the coefficient vector of term $\mathrm{e}^{i\omega T_0}$, denoted as m_1, by solvability conditions, that is, let $< h^*, (m_1, \cos(\frac{nx}{l})) >= 0$, we obtain

$$\frac{\partial G}{\partial T_1} = M\mu G, \tag{3.9}$$

where

$$M = \frac{i(\frac{n}{l})^2d_3v_*\omega h_{11}\mathrm{e}^{-i\omega\tau_c}}{h_{11}\overline{h_{21}} + [-h_{12} - (\frac{n}{l})^2d_3v_*\tau_ch_{11}\mathrm{e}^{-i\omega\tau_c} - gf_2\tau_1h_{12}\mathrm{e}^{-i\omega\tau_1} - gf_1\tau_1h_{11}\mathrm{e}^{-i\omega\tau_1}]\overline{h_{22}}}.$$

Suppose the solution of Eq.(3.8) as follows,

$$\begin{cases} u_2 = \displaystyle\sum_{k=0}^{+\infty}\big(\eta_{0k}G\overline{G} + \eta_{1k}G^2\mathrm{e}^{2i\omega T_0} + \overline{\eta}_{1k}\overline{G}^2\mathrm{e}^{-2i\omega T_0}\big)\cos\Big(\frac{kx}{l}\Big), \\ v_2 = \displaystyle\sum_{k=0}^{+\infty}\big(\zeta_{0k}G\overline{G} + \zeta_{1k}G^2\mathrm{e}^{2i\omega T_0} + \overline{\zeta}_{1k}\overline{G}^2\mathrm{e}^{-2i\omega T_0}\big)\cos\Big(\frac{kx}{l}\Big). \end{cases} \tag{3.10}$$

Denote

$$\begin{cases} e_k =< \cos(\frac{nx}{l}), \cos(\frac{nx}{l}), \cos(\frac{kx}{l}) >= \int_0^{l\pi}\cos^2(\frac{nx}{l})\cos(\frac{kx}{l})dx = \begin{cases} \dfrac{l\pi}{2}, k = 0, \\ \dfrac{l\pi}{4},\ k = 2n \neq 0, \\ 0, k \neq 2n \neq 0, \end{cases} \\ f_k =< \cos(\frac{kx}{l}), \cos(\frac{kx}{l}) >= \int_0^{l\pi}\cos(\frac{kx}{l})\cos(\frac{kx}{l})dx = \begin{cases} l\pi, k = 0, \\ \dfrac{l\pi}{2}, k \neq 0. \end{cases} \end{cases}$$

Substituting solutions given by Eq.(3.7) and Eq.(3.10) into the right-hand side of Eq.(3.8), we obtain

$$\begin{aligned}
\eta_{1k} &= \frac{C_{1k}E_{1k} - B_{1k}F_{1k}}{A_{1k}E_{1k} - B_{1k}D_{1k}},\\
\zeta_{1k} &= \frac{C_{1k}D_{1k} - A_{1k}F_{1k}}{B_{1k}D_{1k} - A_{1k}E_{1k}},\\
\eta_{0k} &= \frac{C_{0k}E_{0k} - B_{0k}F_{0k}}{A_{0k}E_{0k} - B_{0k}D_{0k}},\\
\zeta_{0k} &= \frac{C_{0k}D_{0k} - A_{0k}F_{0k}}{B_{0k}D_{0k} - A_{0k}E_{0k}},
\end{aligned}$$

where

$$\begin{cases}
A_{1k} =2i\omega + d_1 - \Big(r - f_1 - \dfrac{u_*}{K}\Big),\\
B_{1k} =f_2,\\
C_{1k} =\Big(- \dfrac{1}{2}f_{11}h_{11}^2 - f_{12}h_{11}h_{12}\Big)\dfrac{e_k}{f_k},\\
D_{1k} =- d_3v_*\Big(\dfrac{k}{l}\Big)^2\mathrm{e}^{-2i\omega\tau_c} - gf_1\mathrm{e}^{-2i\omega\tau_1},\\
E_{1k} =2i\omega + d_2\Big(\dfrac{k}{l}\Big)^2 - gf_2\mathrm{e}^{-2i\omega\tau_1} + d,\\
F_{1k} =\Big[2d_3\Big(\dfrac{n}{l}\Big)^2h_{11}h_{12}\mathrm{e}^{-i\omega\tau_c} + \dfrac{g}{2}f_{11}h_{11}^2\mathrm{e}^{-2i\omega\tau_1} + gf_{12}h_{11}h_{12}\mathrm{e}^{-2i\omega\tau_1}\Big]\dfrac{e_k}{f_k},\\
A_{0k} =d_1\Big(\dfrac{k}{l}\Big) - \Big(r - f_1 - \dfrac{u_*}{K}\Big),\\
B_{0k} =f_2,\\
C_{0k} =\Big[- f_{11}h_{11}\overline{h_{11}} - f_{12}\Big(h_{11}\overline{h_{12}} + \overline{h_{11}}h_{12}\Big)\Big]\dfrac{e_k}{f_k},\\
D_{0k} =- d_3v_*\Big(\dfrac{k}{l}\Big)^2 - gf_1,\\
E_{0k} =d_2\Big(\dfrac{k}{l}\Big)^2 - gf_2 + d,\\
F_{0k} =2d_3\Big(\dfrac{n}{l}\Big)^2\big[\overline{h_{11}}h_{12}\mathrm{e}^{i\omega\tau_c} + h_{11}\overline{h_{12}}\mathrm{e}^{i\omega\tau_c} + gf_{11}h_{11}^2h_{11}\overline{h_{11}} + gf_{12}(h_{11}\overline{h_{12}}\\
\qquad + \overline{h_{11}}h_{12})\big]\dfrac{e_k}{f_k}.
\end{cases}$$

Especially,

$$\begin{aligned}
\eta_{10} &= \frac{C_{10}E_{10} - B_{10}F_{10}}{A_{10}E_{10} - B_{10}D_{10}},\\
\zeta_{10} &= \frac{C_{10}D_{10} - A_{10}F_{10}}{B_{10}D_{10} - A_{10}E_{10}},\\
\eta_{00} &= \frac{C_{00}E_{00} - B_{00}F_{00}}{A_{00}E_{00} - B_{00}D_{00}},\\
\zeta_{00} &= \frac{C_{00}D_{00} - A_{00}F_{00}}{B_{00}D_{00} - A_{00}E_{00}},
\end{aligned}$$

where

$$\begin{cases} A_{10} = 2i\omega - r + f_1 + 2\dfrac{u_*}{K}, \\ B_{10} = f_2, \\ C_{10} = -\dfrac{1}{4}f_{11}h_{11}^2 - \dfrac{f_{12}}{2}h_{11}h_{12}, \\ D_{10} = -gf_1, \\ E_{10} = 2i\omega - gf_2 + d, \\ F_{10} = \dfrac{g}{4}f_{11}h_{11}^2\mathrm{e}^{-2i\omega\tau_1} + \dfrac{g}{2}f_{12}h_{11}h_{12}\mathrm{e}^{-2i\omega\tau_1}, \\ A_{00} = -r + f_1 + 2\dfrac{u_*}{K}, \\ B_{00} = f_2, \\ C_{00} = -\dfrac{1}{2}f_{11}h_{11}\overline{h_{11}} - \dfrac{f_{12}}{2}(h_{11}\overline{h_{12}} + \overline{h_{11}}h_{12}), \\ D_{00} = -gf_1, \\ E_{00} = -gf_2 + d, \\ F_{00} = \dfrac{g}{2}f_{11}h_{11}\overline{h_{12}} + \dfrac{g}{2}f_{12}h_{11}\overline{h_{12}} + \overline{h_{11}}h_{12}. \end{cases}$$

For ε^3, we obtain

$$\begin{cases} \quad D_0u_3 - d_1u_{xx,3} - \Big(r - f_1 - \dfrac{u_*}{K}\Big)u_3 + \dfrac{u_*}{K}\widetilde{u_3} + f_2v_3 + \dfrac{1}{6}f_{111}u_3^3 \\ = -D_2u_1 - D_1u_2 - \dfrac{\widetilde{u_1}v_2 + \widetilde{u_2}v_1}{K} - f_{11}u_1u_2 - f_{12}u_2v_1 - \dfrac{1}{2}f_{112}u_1^2v_1 + o(\mu), \\ \quad D_0v_3 - d_2v_{xx,3} + d_3v_*u_{xx,3,\tau_c} - gf_2v_{3,\tau_1} - gf_1u_{3,\tau_1} + dv_3 \\ = d_3(u_{xx,2,\tau_c}v_1 - \mu D_0u_{xx,1,\tau_c}v_1 - \tau_cD_1u_{xx,1,\tau_c}v_1) - d_3v_*(-\mu D_0u_{xx,2,\tau_c} \\ \quad - \mu D_1u_{xx,1,\tau_c} - \tau_cD_2u_{xx,1,\tau_c} - \tau_cD_1u_{xx,2,\tau_c}) - d_3(u_{x,2,\tau_c}v_{x,1} - \mu D_0u_{xx,1,\tau_c} \\ \quad - \tau_cD_1u_{xx,1,\tau_c}v_1) + gf_2(-\tau_1D_1v_{2,\tau_1} - \tau_1^2D_2v_{1,\tau_1}) + gf_1(\tau_1D_1u_{2,\tau_1} + \tau_1^2D_2u_{1,\tau_1}) \\ \quad + gf_{11}(u_{2,\tau_1}u_{1,\tau_1} - \tau_1D_1u_{1,\tau_1}u_{1,\tau_1}) + gf_{12}(u_{2,\tau_1}v_{1,\tau_1} - \tau_1D_1u_{1,\tau_1}v_{1,\tau_1} + u_{1,\tau_1}v_{2,\tau_1} \\ \quad - \tau_1D_1v_{1,\tau_1}u_{1,\tau_1}) + \dfrac{g}{6}f_{111}u_{1,\tau_1}^3 + \dfrac{g}{2}f_{112}u_{1,\tau_1}^2v_{1,\tau_1} + o(\mu). \end{cases} \tag{3.11}$$

Substituting solutions from Eq.(3.7) and Eq.(3.10) into the right-hand side of Eq.(3.11), we obtain the coefficient vector of term $e^{i\omega T_0}$, denoted as m_2. By solvability conditions, let $< h^*, (m_2, \cos(\frac{nx}{l})) >= 0$, and we obtain

$$\frac{\partial G}{\partial T_2} = XG^2\overline{G}, \tag{3.12}$$

where

$$X = \frac{h_{21}X_{11} - h_{22}X_{12}}{(-h_{21}h_{11} + h_{22}X_{21})f_n},$$

with

$$
\begin{cases}
X_{11} =\dfrac{1}{K}\eta_{00}h_{12}e_0 + \dfrac{1}{K}\eta_{10}\overline{h_{12}}e_0 + f_{11}h_{11}(\eta_{00}e_0+\eta_{02n}e_{2n}) + f_{11}\overline{h_{11}}(\eta_{10}e_0\\
\qquad +\eta_{12n}e_{2n}) + f_{12}h_{11}(\zeta_{00}e_0+\zeta_{02n}e_{2n}) + f_{12}\overline{h_{11}}(\zeta_{10}e_0+\zeta_{12n}e_{2n})\\
\qquad + f_{12}h_{12}(\eta_{00}e_0+\eta_{02n}e_{2n}) + f_{12}\overline{h_{12}}(\eta_{10}e_0+\eta_{12n}e_{2n})\\
\qquad + \dfrac{1}{2}f_{112}h_{11}^2\overline{h_{12}}\displaystyle\int_0^{l\pi}\cos^4\Big(\frac{nx}{l}\Big)dx + f_{112}h_{11}\overline{h_{11}}h_{12}\int_0^{l\pi}\cos^4\Big(\frac{nx}{l}\Big)dx,\\
X_{12} =d_3h_{12}\Big(\dfrac{2n}{l}\Big)^2(\eta_{00}e_0+\eta_{02n}e_{2n}) + d_3\overline{h_{12}}\Big(\frac{k}{l}\Big)^2(\eta_{10}e_0+\eta_{12n}e_{2n})\\
\qquad - d_3\dfrac{n}{l}h_{12}\Big(\dfrac{2n}{l}\Big)(\eta_{00}+\eta_{02n})\displaystyle\int_0^{l\pi}\sin\Big(\frac{nx}{l}\Big)\cos\Big(\frac{nx}{l}\Big)\sin\Big(\frac{kx}{l}\Big)dx\\
\qquad - d_3\dfrac{n}{l}\overline{h_{12}}\mathrm{e}^{-2i\omega\tau_c}\Big(\dfrac{2n}{l}\Big)\eta_{12n}\displaystyle\int_0^{l\pi}\sin\Big(\frac{nx}{l}\Big)\cos\Big(\frac{nx}{l}\Big)\sin\Big(\frac{kx}{l}\Big)dx\\
\qquad + gf_{11}h_{11}\mathrm{e}^{-i\omega\tau_1}(\eta_{00}e_0+\eta_{02n}e_{2n}) + gf_{11}h_{11}\mathrm{e}^{-i\omega\tau_1}(\eta_{10}e_0+\eta_{12n}e_{2n})\\
\qquad + gf_{12}h_{12}\mathrm{e}^{-i\omega\tau_1}(\eta_{00}e_0+\eta_{02n}e_{2n}) + gf_{12}h_{12}\mathrm{e}^{-i\omega\tau_1}(\eta_{10}e_0+\eta_{12n}e_{2n})\\
\qquad + gf_{12}h_{11}\mathrm{e}^{-i\omega\tau_1}(\zeta_{00}e_0+\zeta_{02n}e_{2n}) + gf_{12}\overline{h_{11}}\mathrm{e}^{-i\omega\tau_1}(\zeta_{10}e_0+\zeta_{12n}e_{2n})\\
\qquad + \dfrac{g}{2}f_{111}h_{11}^2\overline{h_{11}}\mathrm{e}^{-i\omega\tau_1}\displaystyle\int_0^{l\pi}\cos^4\Big(\frac{nx}{l}\Big)dx\\
\qquad + gf_{112}h_{11}\overline{h_{11}}h_{12}\mathrm{e}^{-i\omega\tau_1}\displaystyle\int_0^{l\pi}\cos^4\Big(\frac{nx}{l}\Big)dx\\
\qquad + \dfrac{g}{2}f_{112}h_{11}^2\overline{h_{12}}\mathrm{e}^{-i\omega\tau_1}\displaystyle\int_0^{l\pi}\cos^4\Big(\frac{nx}{l}\Big)dx,\\
X_{21} =-d_3v_*\Big(\dfrac{n}{l}\Big)^2\tau_c\mathrm{e}^{-i\omega\tau_c}h_{11} - gf_2\tau_1^2\mathrm{e}^{-i\omega\tau_c}h_{12} + gf_1\tau_1^2\mathrm{e}^{-i\omega\tau_1}h_{11}.
\end{cases}
$$

According to the above analysis, the normal form of Hopf bifurcation for model (1.2) reduced on the center manifold is

$$\dot{G} = M\mu G + XG^2\overline{G}, \tag{3.13}$$

where M and X are given by Eq.(3.9) and Eq.(3.12), respectively.

Let $G = re^{i\theta}$ and substitute it into Eq.(3.13), and we obtain the Hopf bifurcation normal form in polar coordinates:

$$\begin{cases}\dot{r} = \mathrm{Re}(M)\mu r + \mathrm{Re}(X)r^3,\\ \dot{\theta} = \mathrm{Im}(M)\mu + \mathrm{Im}(X)r^2.\end{cases} \tag{3.14}$$

Therefore, we have the following theorem.

Theorem 3.1. *For system* (3.14), *if* $\frac{\mathrm{Re}(M)\mu}{\mathrm{Re}(X)} < 0$ *holds, there exist periodic solutions near the constant steady state* $E_1 = (u_*, v_*)$ *in model* (1.2).

(i) If $\mathrm{Re}(M)\mu < 0$, *the bifurcating periodic solutions reduced on the center manifold are unstable, and the direction of bifurcation is forward (backward) for* $\mu > 0$ $(\mu < 0)$;

(ii) If $\mathrm{Re}(M)\mu > 0$, *the bifurcating periodic solutions reduced on the center manifold are stable, and the direction of bifurcation is forward (backward) for* $\mu > 0$ $(\mu < 0)$.

Proof. A nontrivial equilibrium point of model (3.14) corresponds to a periodic solution of model (1.2). When $\frac{\mathrm{Re}(M)\mu}{\mathrm{Re}(X)} < 0$, the nontrivial steady state of model (3.14) is given by

$$\hat{r} = \sqrt{\frac{-\mathrm{Re}(M)\mu}{\mathrm{Re}(X)}}.$$

Moreover, $(\mathrm{Re}(M)\mu + 3\mathrm{Re}(X)r^2)|_{r=\hat{r}} = -2\mathrm{Re}(M)\mu$. According to the stability theory of steady states, if $\mathrm{Re}(M)\mu < 0$, then the corresponding periodic solution is unstable.

□

Remark 3.1. In the derivation of the normal form of the Hopf bifurcation for model (1.2), we initially considered the case where both $\tau_1 \neq 0$ and $\tau_2 \neq 0$, applying the standard multiple time scales method. This approach is general and applicable to various situations as long as the bifurcation conditions are met. In particular, when $\tau_2 = 0$, the same derivation remains valid and the results directly follow, with no additional complexities. Thus, the method can be applied without restriction, regardless of whether τ_1 or τ_2 is zero.

4. Numerical simulations

In this section, we review relevant literature to determine appropriate parameter values for the pest models. We select different habitat complexities for comparison to explore their effects on gestation delay and memory period and perform numerical simulations to verify the correctness of the theoretical analysis.

4.1. Selection of parameter values

In this subsection, we perform data analysis to determine parameter values for simulations.

(i) Death rate of predator d.
From [25], Picoides major, a type of insectivorous bird, is mentioned as a predator of insects, with a death rate of 0.426. In a relatively closed environment, human factors and external intrusions are relatively low. Based on the above, the natural mortality rate of animals can be reduced, and we select the death rate $d = 0.3$ for the predatory natural enemy of the Dendrolimus superans.

(ii) Attack rate of predator on prey a and energy transfer efficiency g.
In experimental interventions, the attack rate of sparrow hawk ranges from 0.6 to 1 [26]. However, returning to real-life scenarios, the actual predation rate by predators, influenced by multiple factors such as natural environment and prey evasion, is lower than this range. Therefore, we select $a = 0.6$. From [27], the conversion efficiency of birds for insects ranges from 0.54 to 0.75. Therefore, we adopt an energy transfer efficiency $g = 0.6$.

(iii) Diffusion coefficients d_1, d_2, d_3.
Compared with their predatory natural enemy insectivorous bird, the mobility of Dendrolimus superan larvae and adults is relatively slow. Therefore, we set the diffusion coefficient of Dendrolimus superans $d_1 = 0.01$ and diffusion coefficient of insectivorous birds $d_2 = 0.2$. When predators detect prey, their instinctual memory prompts an increase in their movement speed towards the direction of the prey. Hence, we set the coefficient of memory diffusion $d_3 = 0.05$.

(iv) Habitat complexity c.
From [28], different habitat complexities have a significant impact on the macroinvertebrate richness in the environment, as well as on population density. The phenomena caused by varying habitat complexities also differ greatly. Therefore, we select two groups with different habitat complexity for our study: one with $c_1 = 0.55$ and the other with $c_2 = 0.3$.

(v) Other dimensionless parameters r, K, h.
Dendrolimus superans lays an average of 260 eggs per female, completing egg-laying in two to three batches. The female-to-male ratio is approximately 1.5, and they have a biennial generation period. Therefore, we take the birth rate $r = 0.42$. Considering the outbreak years of Dendrolimus superan, the birth rate can also be slightly increased. For the environmental capacity of Dendrolimus superans, we set $K = 5$. Additionally, for the handling time of predators for prey, we choose $h = 0.41$ for the simulations.

To summarize the above analysis, we choose $d = 0.3$, $a = 0.6$, $g = 0.6$, $d_1 = 0.01$, $d_2 = 0.2$, $d_3 = 0.05$, $r = 0.42$, $K = 5$ and $h = 0.41$.

4.2. Simulations

In this section, we perform numerical simulations for model (1.2). The simulation results can serve as a reference for preventing and controlling outbreaks of Dendrolimus superans, providing a theoretical basis. When $l = 1$, we have $rhdl^2 - (d_1 + d_2)g < 0$. Due to $\frac{hd+g}{ahK(g-hd)} = 1.2323$, $\frac{d_3 g}{hd_2 a(g-hd)} = 1.2783$, $c_0 = 1.2323$, that is when $c < 1.2323$, (H_1) always holds. In the following sections, we will analyze the possible dynamic phenomena that might occur under two different habitat complexities.

Case 1: $c = c_1 = 0.55$

With the above parameters, when $c = c_1 = 0.55$, (H_0) holds and the model (1.2) has a positive constant steady state $E_1 = (1.9059, 0.9907)$.

When $\tau_1 = 0$, $\tau_2 = 0$, (H_1) holds, according to Theorem 2.1, then the positive constant steady state E_1 of the model (1.2) is locally asymptotically stable. This means that if the model (1.2) is without delays, although predatory birds and Dendrolimus superan can coexist at this time, natural predators can suppress the reproduction of pests. In this condition, we assume that predators do not have gestation delays or memory period.

When $\tau_1 \neq 0$, $\tau_2 = 0$, by a simple calculation, $I_1 \neq \emptyset$ only holds for $n = 1$ and there does not exist any n such that $I_2 \neq \emptyset$ holds. Thus, Eq.(2.6) has a unique positive root $\omega_1 = 0.1935$, where ω_1 corresponds to the critical delay $\tau_{1,1}^{(0)} = 2.7972$. Based on the definition of $\tau_{1,c}^*$ given in Eq.(2.7), we choose $\tau_{1,c}^* = 2.7972$. According

to Theorem 2.2, we can conclude that the positive constant steady state E_1 is locally asymptotically stable for $\tau_1 = 1.6 \in [0, 2.7972)$; see Fig.3.

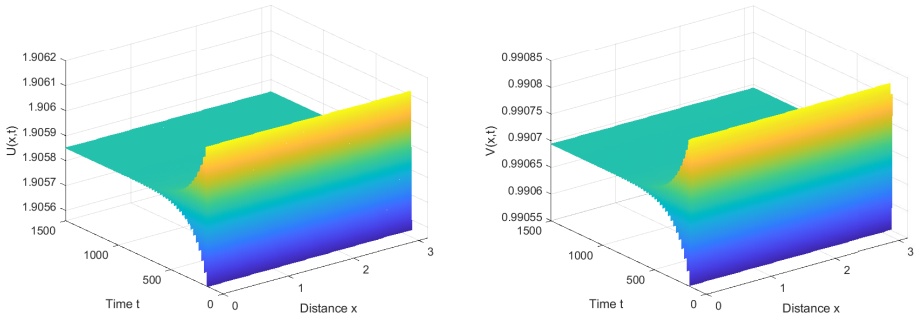

(a) (b)

Figure 3. Simulated solution of model (1.2) for $\tau_1 = 1.6, \tau_2 = 0$, showing a locally asymptotically stable positive constant steady state E_1.

We choose $\tau_1 = 2.8 > \tau_{1,c}^* = 2.7972$. From Eq.(3.9) and Eq.(3.12), we obtain $\mathrm{Re}(M) > 0$, $\mathrm{Re}(X) < 0$. Thus, according to Theorem 2.2 and Theorem 3.1, the model (1.2) will generate inhomogeneous periodic solutions near the positive constant steady state E_1 of model (1.2), and bifurcating periodic solutions are stable and forward; see Fig.4.

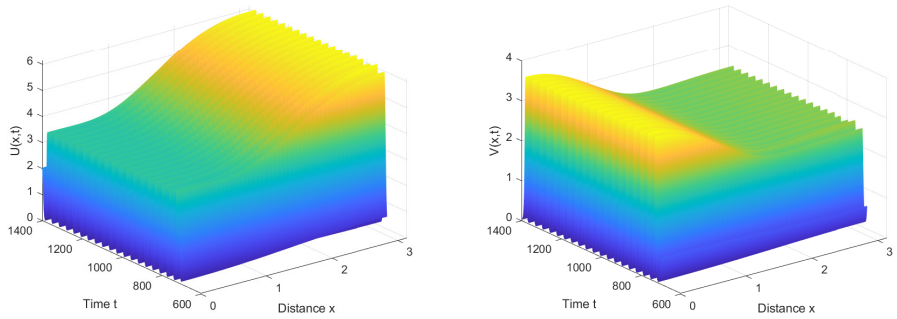

(a) (b)

Figure 4. Model (1.2) generates inhomogeneous stable and forward periodic solutions for model (1.2) near E_1 for $\tau_1 = 2.8, \tau_2 = 0$.

Biological interpretation 1:

(i) Under the premise of predators having no memory period, when the gestation period of predators is below the critical value $\tau_{1,c}^*$, rapid pursuit of predators based on memory quickly controls the population of the Dendrolimus superans and reaches a stable state;

(ii) When gestation period is slightly above the critical value $\tau_{1,c}^*$, natural enemies exert a certain degree of control over the population of Dendrolimus superan, but they cannot effectively suppress the reproduction of pests. Consequently, there is a characteristic of periodic outbreaks in pest formation. In the cyclical

prevention and control of pests, the population of natural enemies also shows periodic growth. When insectivorous birds have a longer gestation delay, human intervention is necessary for pest control. We can release insectivorous birds to increase their numbers, indirectly reducing the negative effects caused by the predators' prolonged gestation period, thus bringing pest levels back to a controllable and stable state.

When $\tau_2 \neq 0, \tau_1 \neq 0$, since $I_1 \neq \emptyset$ and $I_2 = \emptyset$, denote the first stable interval mentioned in Theorem 2.2 as $I = (0, 2.7972)$, on which the equilibrium E_1 is locally asymptotically stable for $\tau_2 = 0$. When $n = 1, 2, 3$, $I_3 \neq \emptyset$. We choose $\tau_1 = 1.6 \in I$, thus, Eq.(2.12) has two positive roots $\omega_{1,1} = 0.2185$ and $\omega_{1,2} = 0.1366$ for $n = 1$, where $\omega_{1,1}$ corresponds to the critical delay $\tau^{(0)}_{2,1,1} = 2.4268$, and $\omega_{1,2}$ corresponds to the critical delay $\tau^{(0)}_{2,1,2} = 21.1661$, and Eq.(2.12) has only one positive root for $n = 2, 3$. Further more, we have

$$0 < \tau^{(0)}_{2,1,1} = 2.4268 < \tau^{(0)}_{2,2} = 12.6640 < \tau^{(0)}_{2,3} = 18.8755 < \tau^{(0)}_{2,1,2} = 21.1661 < \cdots,$$

and

$$\mathrm{Re}\Big(\frac{d\lambda}{d\tau_2}\Big)^{-1}_{\tau_2=2.4268} > 0, \ \mathrm{Re}\Big(\frac{d\lambda}{d\tau_2}\Big)^{-1}_{\tau_2=12.6640} > 0.$$

From the definition of τ_c, we choose $\tau_c = 2.4268$. According to Theorem 2.3, we can conclude that the positive constant steady state E_1 is locally asymptotically stable for $\tau_2 \in [0, 2.4268)$ and unstable for $\tau_2 \in (2.4268, +\infty)$. The positive constant steady state E_1 is asymptotically stable for $\tau_2 = 1.5 \in [0, 2.4268)$; see Fig.5.

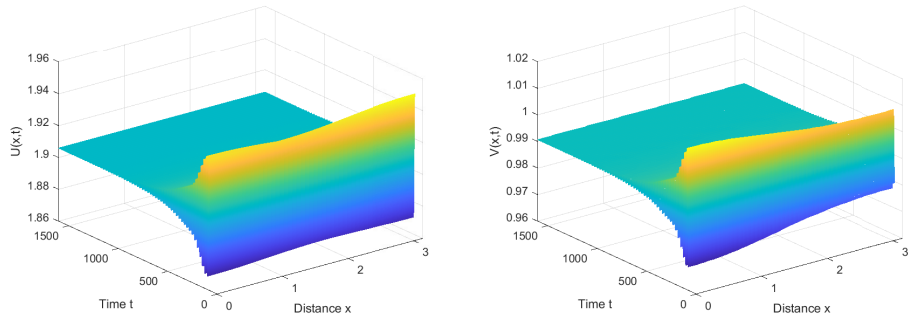

(a) (b)

Figure 5. Simulated solution of model (1.2) for $\tau_1 = 1.6, \tau_2 = 1.5$, showing a locally asymptotically stable positive constant steady state E_1.

We choose $\tau_2 = 4 > \tau_c = 2.4268$. From Eq.(3.9) and Eq.(3.12), we obtain $\mathrm{Re}(M) > 0$, $\mathrm{Re}(X) < 0$. Thus, according to Theorem 2.3 and Theorem 3.1, the model (1.2) will generate inhomogeneous periodic solutions near the positive constant steady state E_1 of model (1.2), and bifurcating periodic solutions are stable and forward; see Fig.6.

Biological interpretation 2:

(i) When the gestation delay and memory period of insectivorous birds are both below the critical values $\tau^*_{1,c}$ and τ_c, the population of pests is efficiently sup-

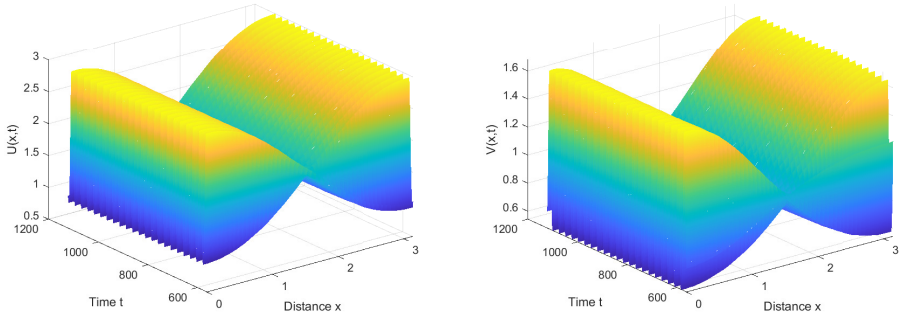

(a) (b)

Figure 6. Model (1.2) generates inhomogeneous stable and forward periodic solutions for model (1.2) near E_1 for $\tau_1 = 1.6, \tau_2 = 4$.

pressed. At this point, the damage caused by forest pests is effectively controlled through physical interventions;

(ii) Under the premise that the gestation period of predators is below the critical value $\tau^*_{1,c}$, when memory period is slightly above the critical value τ_c, predators have a longer memory period, and their ability to hunt prey decreases, leading to reduced food sources for predators. This also results in a decline in the reproductive capacity of prey populations. The decrease in predator numbers causes outbreaks of Dendrolimus superans populations. However, competition among Dendrolimus superans populations leads to a reduction in their numbers due to food scarcity once they reach a certain density. This cyclic increase in population densities of both predators and caterpillars makes pest control difficult to manage effectively;

(iii) We find that when habitat complexity is high, populations exhibit a uniform distribution in single-delay systems, while they display a bimodal distribution in double-delay systems. This is because, in systems with higher habitat complexity, animals choose suitable areas based on varying habitat conditions. In the context of single-delay systems, the survival pressure on predators is relatively low, and reduced interspecies competition results in a uniform population distribution. However, in double-delay systems, the increased survival pressure on predators leads them to select suitable habitats under different conditions. This stronger interspecies competition causes the population to exhibit a bimodal distribution.

Case 2: $c = c_2 = 0.3$

When $c = c_2 = 0.3$, the model (1.2) has a positive constant steady state $E_1 = (3.4941, 0.8840)$. Following the same steps as above, we can obtain $\tau^{(0)}_{1,1} = 11.5065$ at $n = 1$ and $\tau^{(0)}_{2,2} = 14.1681$ at $n = 2$. From the definition of $\tau^*_{1,c}$ and τ_c, we choose $\tau^*_{1,c} = 11.5065$ and $\tau_c = 4.5746$.

When $\tau_1 \neq 0$, $\tau_2 = 0$, according to Theorem 2.2, we can conclude that the positive constant steady state E_1 is locally asymptotically stable for $\tau_1 = 4 \in [0, 11.5065)$; see Fig.7.

We choose $\tau_1 = 12 > \tau^*_{1,c} = 11.5065$. From Eq.(3.9) and Eq.(3.12), we obtain $\mathrm{Re}(M) > 0$, $\mathrm{Re}(X) < 0$. Thus, according to Theorem 2.2 and Theorem 3.1, the

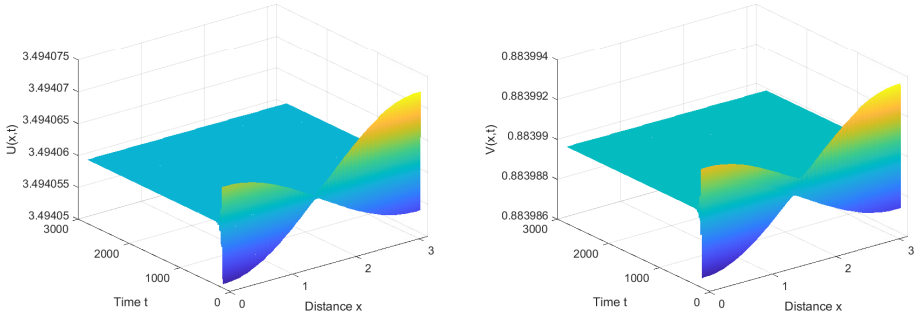

(a) (b)

Figure 7. Simulated solution of model (1.2) for $\tau_1 = 4, \tau_2 = 0$, showing a locally asymptotically stable positive constant steady state E_1.

model (1.2) will generate inhomogeneous periodic solutions near the positive constant steady state E_1 of model (1.2), and bifurcating periodic solutions are stable and forward; see Fig.8.

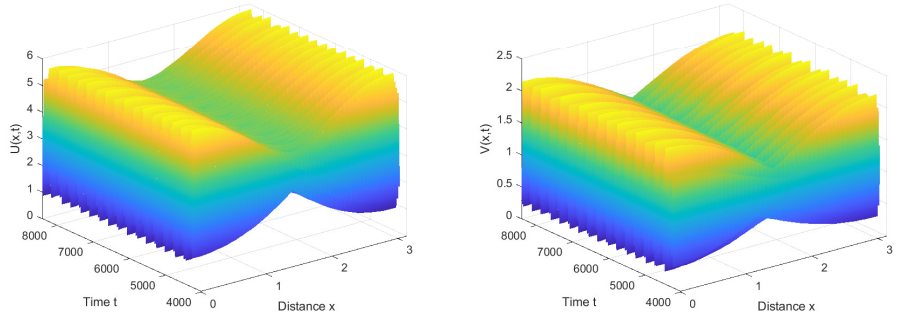

(a) (b)

Figure 8. Model (1.2) undergoes inhomogeneous stable and forward periodic solutions of Hopf bifurcation near E_1 for $\tau_1 = 12, \tau_2 = 0$.

When $\tau_1 \neq 0$, $\tau_2 \neq 0$, denote the first stable interval mentioned in Theorem 2.2 as $I = (0, 11.5065)$, and choose $\tau_1 = 4 \in I$. According to Theorem 2.3, we can conclude that the positive constant steady state E_1 is locally asymptotically stable for $\tau_2 \in [0, 4.5746)$ and unstable for $\tau_2 \in (4.5746, +\infty)$. The positive constant steady state E_1 is locally asymptotically stable for $\tau_2 = 3.5 \in [0, 4.5746)$; see Fig.9.

We choose $\tau_2 = 4.6 > \tau_c = 4.5746$. From Eq.(3.9) and Eq.(3.12), we obtain $\mathrm{Re}(M) > 0$, $\mathrm{Re}(X) < 0$. Thus, according to Theorem 2.3 and Theorem 3.1, the model (1.2) will generate inhomogeneous periodic solutions near the positive constant steady state E_1 of model (1.2), and bifurcating periodic solutions are stable and forward; see Fig.10.

Biological interpretation 3:
When habitat complexity decreases, the reduction in environmental resources

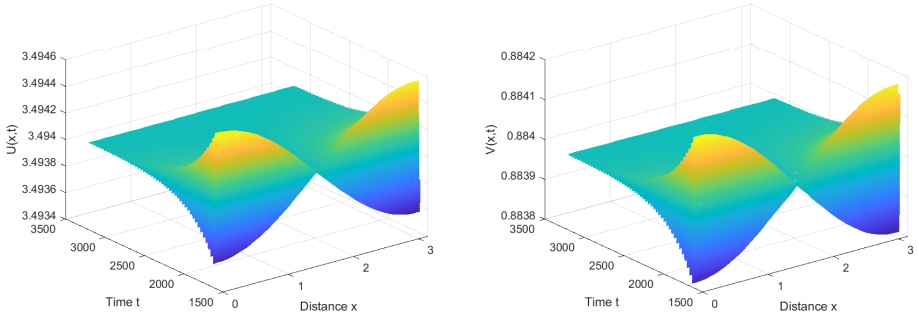

(a) (b)

Figure 9. Simulated solution of model (1.2) for $\tau_1 = 4, \tau_2 = 3.5$, showing a locally asymptotically stable positive constant steady state E_1.

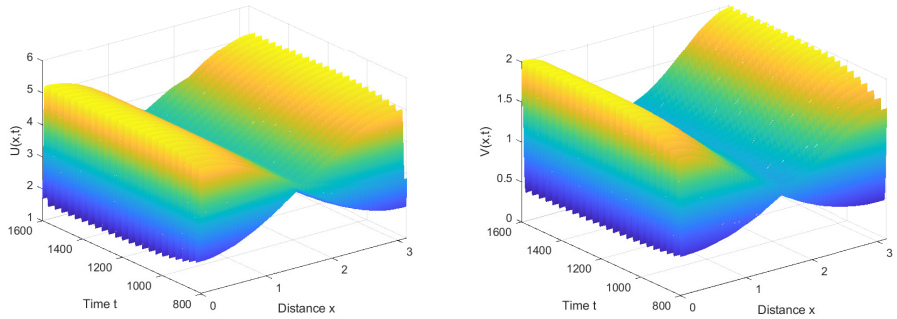

(a) (b)

Figure 10. Model (1.2) undergoes inhomogeneous stable and forward periodic solutions of Hopf bifurcation near E_1 for $\tau_1 = 4, \tau_2 = 4.6$.

typically leads to changes in the gestation delay of predators to adapt to resource fluctuations. In environments with lower habitat complexity, pure larch forests provide a more suitable environment for the breeding and growth of Dendrolimus superans, thereby increasing the abundance of prey for predators. This necessitates a longer gestation delay for predators to exhibit periodic outbreaks of pests. However, in habitats with lower complexity, the memory period of animals tends to show less variation because lower habitat complexity facilitates quicker adaptation of animals to the environment.

Remark 4.1. By contrasting different levels of habitat complexity, we observe that increasing habitat complexity effectively suppresses and stabilizes the population density of Dendrolimus superans over a relatively short period. Additionally, in terms of spatial distribution, lower habitat complexity leads to an uneven distribution of natural enemies and Dendrolimus superans, whereas higher habitat complexity results in a more uniform distribution. The uneven distribution of Dendrolimus superans makes pest control more challenging and prolongs the treatment period. Constructing mixed forests is a common approach to enhancing habitat complexity and managing Dendrolimus superans infestations [29].

Remark 4.2. Moreover, under the given parameter settings, when the habitat complexity parameter $c \geq 0.7563$, the model (1.2) exhibits spatially homogeneous periodic solutions irrespective of the presence of the nonlocal competition term. Under such conditions, the nonlocal effect does not influence the qualitative dynamics of the system. When $0.5576 \leq c < 0.7563$, the model (1.2) without nonlocal competition shows only spatially homogeneous periodic solutions, while the inclusion of nonlocal competition leads to spatially inhomogeneous periodic solutions. When $c < 0.5576$, the model (1.2) without nonlocal effects remains stable, but with nonlocal competition, spatially inhomogeneous periodic solutions emerge. From a biological perspective, when the habitat is highly complex, the influence of nonlocal competition is negligible. In contrast, when the habitat complexity is moderate to low, nonlocal competition becomes more influential, promoting the emergence of spatial structures in the population.

5. Conclusion

In this paper, considering the Holling II type functional response, we developed a pest control model incorporating two delays and nonlocal competition aimed at controlling the population density of the Dendrolimus superans. We analyzed the existence and stability of the positive constant steady state and the existence of Hopf bifurcations near the positive constant steady state. In the numerical simulation section, we selected an appropriate set of parameters for the simulations. By comparing experimental results obtained with different strength of habitat complexity c, we found that, under the influence of nonlocal competition two delays, the stable inhomogeneous bifurcating periodic solutions of Hopf bifurcation near the positive constant steady state can be derived. We provided biological explanations to demonstrate the feasibility of effectively controlling the population density of the Dendrolimus superans and maintaining a stable and controllable population density level between natural enemies and the Dendrolimus superans, thereby achieving effective environmental protection and true green pest control. When choosing a lower habitat complexity, both time delay critical values in the model increase, leading to changes in the dynamical properties of the model.

The incorporation of two delays further refines the process of biological control. Both the memory period of predators and the gestation delay significantly impact on the effectiveness of pest control. Therefore, we can mitigate these impacts on a smaller scale by implementing targeted interventions to address the negative effects caused by delayed pregnancy and excessive memory periods in predators. This, in turn, can reduce the likelihood of pest outbreaks and restore the population growth of Dendrolimus superans to a controllable and stable state.

References

[1] J. Qin, J. Li, Q. Gao, J. Wilson and A. Zhang, *Mitochondrial phylogeny and comparative mitogenomics of closely related pine moth pests (Lepidoptera: Dendrolimus)*, PeerJ, 2019, 7, e7317.

[2] J. Wang, S. Wu and J. Shi, *Pattern formation in diffusive predator-prey systems with predator-taxis and prey-taxis*, Discrete & Continuous Dynamical Systems-B, 2021, 26(3), 1273–1289.

[3] X. Wang and X. Zou, *Modeling the fear effect in predator-prey interactions with adaptive avoidance of predators*, Bulletin of Mathematical Biology, 2017, 79, 1325–1359.

[4] J. L. Orrock, J. H. Grabowski, J. H. Pantel, S. D. Peacor, B. L. Peckarsky, A. Sih and E. E. Werner, *Consumptive and nonconsumptive effects of predators on metacommunities of competing prey*, Ecology, 2008, 89(9), 2426–2435.

[5] K. Ryu and W. Ko, *Asymptotic behavior of positive solutions to a predator-prey elliptic system with strong hunting cooperation in predators*, Physica A: Statistical Mechanics and Its Applications, 2019, 531, 121726.

[6] T. A. Troost, B. W. Kooi and U. Dieckmann, *Joint evolution of predator body size and prey-size preference*, Evolutionary Ecology, 2008, 22, 771–799.

[7] S. Ruan, *On nonlinear dynamics of predator-prey models with discrete delay*, Mathematical Modelling of Natural Phenomena, 2009, 4(2), 140–188.

[8] J. A. Cousin and R. D. Phillips, *Habitat complexity explains species-specific occupancy but not species richness in a Western Australian woodland*, Australian Journal of Zoology, 2008, 56(2), 95–102.

[9] A. Hauser, M. J. Attrill and P. A. Cotton, *Effects of habitat complexity on the diversity and abundance of macrofauna colonising artificial kelp holdfasts*, Marine Ecology Progress Series, 2006, 325, 93–100.

[10] A. Ossola, M. A. Nash, F. J. Christie, A. K. Hahs and S. J. Livesley, *Urban habitat complexity affects species richness but not environmental filtering of morphologically-diverse ants*, PeerJ, 2015, 3, e1356.

[11] Z. Y. Nangong, J. Yang, X. P. Xu and B. J. Gao, *Morphological diversity of four Dendrolimus species in relation to environmental factors*, Chinese Journal of Ecology, 2013, 32(3), 627.

[12] D. Han, S. Wang, J. Zhang, R. Cui and Q. Wang, *Evaluating Dendrolimus superans (Lepidoptera: Lasiocampidae) occurrence and density modeling with habitat conditions*, Forests, 2024, 15(2), 388.

[13] A. J. Lotka, *Fluctuations in the abundance of a species considered mathematically*, Nature, 1927, 119, 12.

[14] R. G. Pradeep, V. K. Chandrasekar, M. Senthilvelan and M. Lakshmanan, *On certain new integrable second order nonlinear differential equations and their connection with two dimensional Lotka-Volterra system*, Journal of Mathematical Physics, 2010, 51(3), 033519.

[15] J. Giné and V. G. Romanovski, *Integrability conditions for Lotka-Volterra planar complex quintic systems*, Nonlinear Analysis: Real World Applications, 2010, 11(3), 2100–2105.

[16] Z. Ma and S. Wang, *A delay-induced predator-prey model with Holling type functional response and habitat complexity*, Nonlinear Dynamics, 2018, 93, 1519–1544.

[17] S. Wu and Y. Song, *Spatiotemporal dynamics of a diffusive predator-prey model with nonlocal effect and delay*, Communications in Nonlinear Science and Numerical Simulation, 2020, 89, 105310.

[18] Y. Peng and G. Zhang, *Dynamics analysis of a predator-prey model with herd behavior and nonlocal prey competition*, Mathematics and Computers in Simulation, 2020, 170, 366–378.

[19] S. Liu, E. Beretta and D. Breda, *Predator-prey model of Beddington-DeAngelis type with maturation and gestation delays*, Nonlinear Analysis: Real World Applications, 2010, 11(5), 4072–4091.

[20] R. Singh, A. Ojha and N. K. Thakur, *Modeling the effect of interference and gestation delay in an interacting good biomass and bird population: an application to wetland ecosystem*, Thalassas, 2024, 40, 539–556.

[21] X. Zhou, X. Shi and X. Song, *Analysis of nonautonomous predator-prey model with nonlinear diffusion and time delay*, Applied Mathematics and Computation, 2008, 196(1), 129–136.

[22] R. Yang, C. Zhang and Y. Zhang, *A delayed diffusive predator-prey system with Michaelis-Menten type predator harvesting*, International Journal of Bifurcation and Chaos, 2018, 28(08), 1850099.

[23] Y. Lv, *The spatially homogeneous Hopf bifurcation induced jointly by memory and general delays in a diffusive system*, Chaos, Solitons & Fractals, 2022, 156, 111826.

[24] Y. Wang, C. Wang, D. Fan and Y. Chen, *Dynamics of a predator-prey model with memory-based diffusion*, Journal of Dynamics and Differential Equations, 2023.
DOI: https://doi.org/10.1007/s10884-023-10305-y

[25] Y. Zhang and Z. Yang, *Studies on the natural enemies and biocontrol of Monochamus alternatus Hope (Coleoptera: Cerambycidae)*, Plant Protection, 2006, 32(2), 9–14.

[26] R. D. Sparrowe, *Prey-catching behavior in the sparrow hawk*, The Journal of Wildlife Management, 1972, 36(2), 297–308.

[27] D. J. Levey and W. H. Karasov, *Digestive responses of temperate birds switched to fruit or insect diets*, The Auk, 1989, 106(4), 675–686.

[28] J. I. St. Pierre and K. E. Kovalenko, *Effect of habitat complexity attributes on species richness*, Ecosphere, 2014, 5(2), 1–10.

[29] C. L. C. Liu, O. Kuchma and K. V. Krutovsky, *Mixed-species versus monocultures in plantation forestry: Development, benefits, ecosystem services and perspectives for the future*, Global Ecology and Conservation, 2018, 15, e00419.